

Li Wei, Zhang Ming, Zhang Jinli, Han Yongcai

## Self-assembly of cetyl trimethylammonium bromide in ethanol-water mixtures

© Higher Education Press and Springer-Verlag 2006

**Abstract** The critical micelle concentration (CMC) of cetyl trimethylammonium bromide (CTAB) in both water and ethanol-water-mixed solvent was determined using steady-state fluorescence techniques in order to investigate the effect of the self-assembling properties of the surfactant on the template synthesis of porous inorganic materials. Results indicated that the CMC increased with the increase of ethanol concentration in the mixed solvent. The CMC of CTAB is 0.0009 mol/L in water, while it is 0.24 mol/L in ethanol. Furthermore, the dissipative particle dynamics (DPD) was adopted to simulate the aggregation of CTAB in water and ethanol/water mixtures, and the energy difference was calculated for the surfactant tail groups after mixing with the solvent. The simulation results reflected a regularity similar to the experimental data, i.e., tail groups of CTAB interacted more strongly with ethanol than with water, which elucidates the reason that the micelle is difficult to form in ethanol.

**Keywords** dissipative particle dynamics, cetyl trimethylammonium bromide, micelle

Aggregation properties of surfactants play important roles in many fields such as biology, material, chemical engineering and petroleum recovery. The template synthesis of porous inorganic materials is based on the ordered arrangement of particulates directed by surfactant self-assemblies. Because of their amphiphilic property, surfactant molecules can form different types of aggregate structures in solutions, such as spherical, cylindrical, cubic, hexagonal and lamellar phases, etc. Therefore, the morphology of surfactant self-assembled

templates is fundamental to direct the pore structure of inorganic materials. So far, most of the investigations on the surfactant aggregation properties adopted experimental measurements, e.g., XRD [1], NMR [2], STM [3], DLS [4], and fluorescence spectrophotometry [5]. However, the obtained experimental data usually require special analysis based on certain assumptions, except that the XRD patterns can directly reflect structure information of the aggregates.

A recently emerged mesoscopic simulation method provides one possible means to describe the special properties between microscopic molecule- and macroscopic continuum-level by adopting element units that are larger than traditional atomic scale [6–7]. Dissipative particle dynamics (DPD) is a mesoscopic simulation method that is beneficial for investigating the flow behaviors of complex fluids and other colloidal phenomena, such as the phase equilibria of surfactant solutions, the phase separation of copolymer solutions, aggregation properties of surfactant and polymer mixtures, etc. using DPD simulations [8–10]. For instance, Claesson and Fielden [11] studied the interactions between a cationic polyelectrolyte and an anionic surfactant, sodium dodecyl sulfate (SDS), in solutions, and found that the hydrodynamic radius of the multichain aggregates formed by the polymer and surfactant decreased initially but then increased as the SDS concentration was increased. Groot [12] studied the same system using DPD simulations and concluded that the varying tendency of the hydrodynamic radius depended on the adsorption of surfactant micelles onto the long polymer chains.

Porous silica has been synthesized using the self-assembled surfactant, cetyltrimethyl ammonium bromide (CTAB), as the template [13, 14]. In this kind of template synthesis, ethanol is usually adopted as an additive, however, its effect on the CTAB aggregates is not well clear yet. Investigations on the self-assembling property of CTAB in ethanol-water mixed solvent can provide fundamental directions to the template synthesis of nano-materials.

Translated from *Journal of Tianjin University*, 2006, 39(1) (in Chinese)

Li Wei (✉), Zhang Ming, Zhang Jinli, Han Yongcai  
School of Chemical Engineering and Technology, Tianjin University,  
Tianjin 300072, China  
E-mail: liwei@tju.edu.cn

## 1 Experimental

### 1.1 Reagents

CTAB (analytic purity) was obtained from Shanghai Chemicals Co. (China). Pyrene (99%) was from Sigma. Anhydrous ethanol was from TJU Kewei Co. (China).

### 1.2 CMC measurements using Steady-state Fluorescence

Steady-state fluorescence measurements were carried out on a Cary Eclipse (Varian Ltd.) using pyrene as probe. Fluorescence spectra of the solution samples were recorded at the wavelength range of 350–600 nm. The band-passes for excitation and emission were set to 2.5 nm and the temperature was  $(25 \pm 1)^\circ\text{C}$ . A typical fluorescence spectrum of pyrene monomer displays five major structure vibronic peaks (as shown in Fig. 1). The intensity ratio of the first and the third vibrational bands ( $I_1/I_3$ ), defined as ‘hydrophobic index’, was proved to be useful to investigate the surfactant aggregation properties. The  $I_1/I_3$  value can reflect the polarity of the local micro-environment in the aggregates.

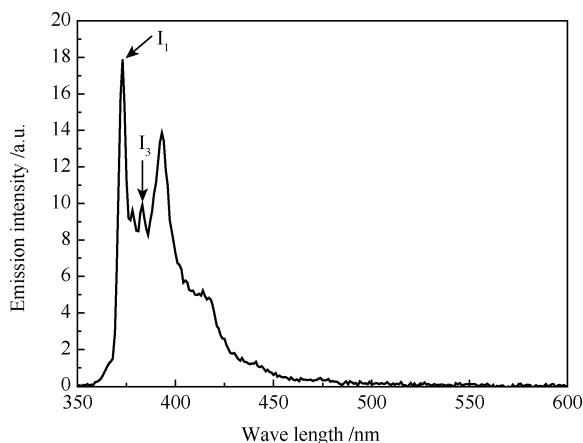


**Fig. 1** Scan spectrum of fluorescence of pyrene in its aqueous solution

### 1.3 DPD simulation

The CTAB molecule was represented by five beads connected with harmonic spring, in which one was the head group, and the other four represented the tail group. Water and ethanol are represented with a single bead respectively.

The interaction parameters  $\alpha_{ij}$  between the head group, the tail group and the solvent molecule can be calculated using Eq. (1),

$$\alpha_{ij} = \frac{\chi_{ij}}{0.306} + 25 \quad (1)$$

where  $\chi_{ij}$  is the Flory-Huggins parameters estimated using the Blends module in Cerius<sup>2</sup> software package (Accelrys Software Inc.). Table 1 lists the calculated values of pa-

rameters  $\alpha_{ij}$ .

All computational works were performed on the SGI Origin3200 workstation. A cubic simulation cell of size  $20 \times 20 \times 20r_C^3$  was used in this work. Different density models were obtained by adding different numbers of surfactant beads into the cell. The initial conformation of the system is produced randomly without constraints, the simulation runs 10000 steps evolving to a steady-state. The temperature was set at 298 K.

**Table 1** Interaction parameters in the simulation system\*

Beads	$\alpha_{ij}$			
	W	H	T	E
W	25.0	15.0	27.8	49.5
H	15.0	25.0	30.0	39.6
T	27.8	30.0	25.0	26.2
E	49.5	39.6	26.2	25.0

\*E represents ethanol, H represents the head group of CTAB, T represents the tail group of CTAB, W represents water.

### 1.4 Solvent effect

To study the effect of solvent composition on the surfactant aggregate properties, the molecular models were established for water, ethanol and CTAB, respectively, and molecular dynamic (MD) simulation was adopted to get the optimized conformation. The energy difference ( $\Delta E$ ) is calculated using Eq. (2),

$$\Delta E = E_{SM} - E_S - E_M \quad (2)$$

where  $E_{SM}$  represents the total energy of the optimal complex consisting of solute and solvent molecules,  $E_M$  is the conformational energy of the solute,  $E_S$  is the energy of the solvent.

The value of  $\Delta E$  reflects the intensity of the interaction between the solute and the solvent molecules. A negative value of  $\Delta E$  indicates that the complex of the solute and the solvent is stable, and the larger the absolute value of  $\Delta E$ , the stronger the interaction is.

## 2 Results and discussion

### 2.1 CMC measurement using steady-state fluorescence

Figure 2 shows the plot of  $I_1/I_3$  of pyrene fluorescence spectra versus the total concentration of CTAB in equal-volume mixed solvent of water and ethanol. No micelles formed in the solution at low CTAB concentration, the corresponding  $I_1/I_3$  is high, which suggests a high polar environment around the pyrene molecule. When the CTAB concentration is higher than CMC, the emerged micelles in solutions result in a low polarity layer around pyrene molecules and make the  $I_1/I_3$  lower.

CMC can be determined via the transition point of the plot of  $I_1/I_3$  versus CTAB concentration. We changed the

solvent composition and measured the corresponding plots of  $I_1/I_3$  versus concentration so as to obtain CMC values of CTAB in different ethanol-water mixtures. Table 2 shows that the CMC of CTAB becomes higher under larger concentration of ethanol, i.e., the increase of ethanol in the solvent mixture results in higher CMC of the surfactant.

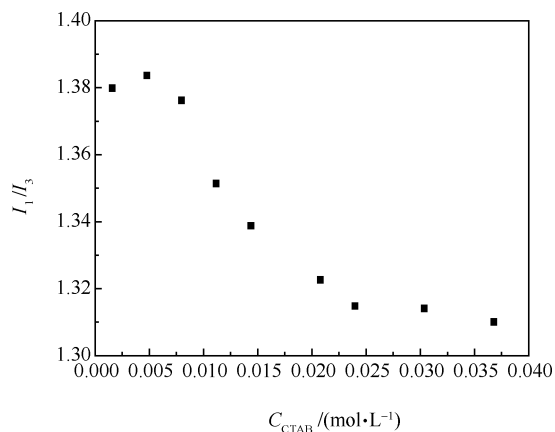


**Fig. 2** Relationship between  $I_1/I_3$  of pyrene and CTAB concentration in an equal-volume mixture of water and ethanol

**Table 2** CMC value of CTAB in ethanol-water mixtures with different volume fraction of ethanol

Fraction of ethanol	CMC ( $\text{mol L}^{-3}$ )
0	0.0009
0.1	0.0015
0.5	0.022
1.0	0.24

## 2.2 DPD simulations of CTAB aggregates

Figure 3 shows the isodensity profiles of the tail group of CTAB in aqueous solutions with different CTAB contents

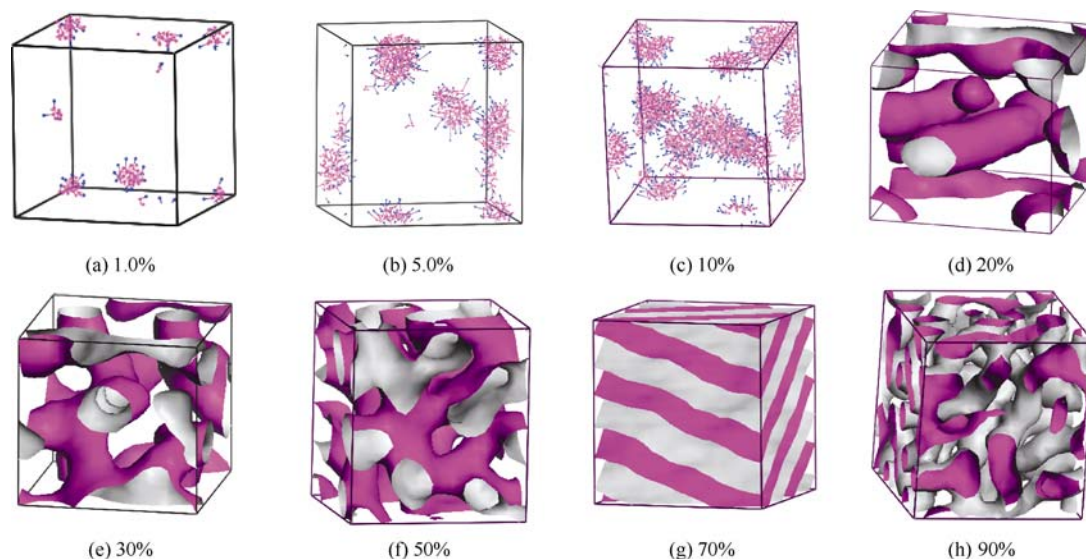


**Fig. 3** Isodensity profiles of surfactant tail in aqueous solutions with different contents of CTAB

after 10000 steps of DPD simulation. As the CTAB content increased, micelles emerged in the solution and the aggregate morphology changed gradually. When the content is as low as 1%, there is only a small amount of spherical micelles of CTAB. Increasing the CTAB content makes collision frequency among these spherical micelles enhanced and gradually merged into elliptical micelles. At high CTAB content the micelles finally transfer into cylindrical shapes. Figures 3(b)–3(e) indicate clearly the evolving process of micelles from spherical to cylindrical shapes, and there is a coexisting period of these two different kinds of micelles. At much higher content CTAB molecules aggregate into hexagonal and even lamellar phases (as shown in Figs. 3g–3h).

The evolution of aggregate morphology along with the surfactant concentration has been confirmed by experimental measurements. For instance, Yuan et al. [10] investigated the micelle morphology of cetyl pyridinium bromide ( $\text{CMC} = 9 \times 10^{-4} \text{ mol/L}$ ) in aqueous solutions by using laser dynamic scattering (ALV/SP-125), and displayed the transformation process of micelles from the spherical to cylindrical shapes together with their coexisting intermediate. Although the CTAB content values used in DPD simulations cannot correspond to the actual concentrations of solutions, it is clear that the DPD simulation is capable of exploring the characteristic transformation of surfactant aggregates.

## 2.3 Effect of ethanol on the aggregate morphology

We carried out DPD simulations of the same content of CTAB (10%) under different solvent compositions in order to study the effect of ethanol on the aggregate in aqueous ethanol solutions. Figure 4 shows the steady-state aggregates in five different solutions. There are obviously large micelles at 10% aqueous CTAB solution. As the ethanol fraction increased in the solvent mixture, the size of micelles decreased gradually. If only ethanol is used as the solvent, there is a small amount of tiny micelles.

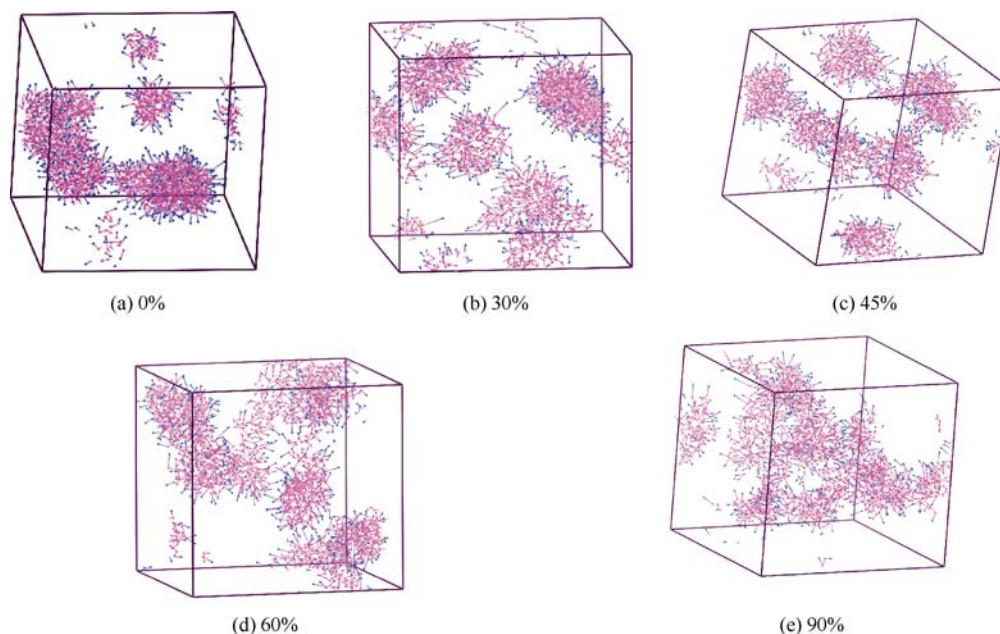


Fig. 4 Aggregates of 10% CTAB in aqueous ethanol solutions with different fractions of ethanol

We further calculated the interaction energy between CTAB molecules and two different solvents using MD simulation. The main driving force of the micelle formation was attributed to the hydrophobic effects among the surfactant tail groups, therefore we compared the interactions between the surfactant tail and the solvent so as to indicate the intensity of hydrophobic effects. Hexadecane molecule was used as the model of CTAB tail group because of the same carbon numbers and the similar structure. Table 3 lists the energy differences of the model molecule in water and ethanol, respectively. In ethanol the value of  $\Delta E$  is  $-170.736$  kJ/mol, while in water it is  $-73.298$  kJ/mol. This suggests that the interaction between the surfactant tail group and ethanol is much stronger, which results in high solubility of hydrophobic molecule in ethanol solution.

Table 3 Optimized energy of the surfactant tail and different solvents

Solvent	$E_M$ (kJ/mol)	$E_S$ (kJ/mol)	$E_{SM}$ (kJ/mol)	$\Delta E$ (kJ/mol)
Water	-184.757	-24415.914	-24673.969	-73.298
Ethanol	-184.757	-16480.515	-16836.008	-170.736

These simulation results are consistent with our experimental data obtained using steady-state fluorescence techniques. Both results indicated that ethanol caused the CMC of CTAB to increase, i.e., it is not so easy for CTAB to form micelles in ethanol as in water.

### 3 Conclusions

(1) CMC values of CTAB in ethanol aqueous solutions were measured using the steady-state fluorescence technique, and it was found that the value of CMC increases as the ethanol

fraction increases in the mixed solvent. The CMC value of CTAB is  $0.0009$  mol/L in water, while it is up to  $0.24$  mol/L<sup>3</sup> in ethanol. (2) DPD simulations were carried out to study the aggregate morphology of CTAB in water and ethanol-water mixed solvent, and MD method was adopted to investigate the interaction energy between the tail group of CTAB and the solvent molecule. DPD simulation results show the evolving process of the aggregates from spherical to cylindrical, hexagonal, and finally lamellar phase. MD calculations indicate that the hydrophobic tail group of CTAB has strong interactions with ethanol, which make the formation of CTAB micelle difficult in ethanol. These simulation results are consistent with our experimental data.

**Acknowledgements** We greatly appreciated the SINOPEC Research Institute of Petroleum Processing, Beijing, for utilizing the simulation software. This work was financially supported by the National Natural Science Foundation of China (Grant No. 20306023) and the Sinopec (X502012).

### References

1. Brown S.P., Schnell I., Brand J.D., Müllen K., Spiess H.W., An Investigation of  $\pi$ - $\pi$  Packing in a Columnar Hexabenzocoronene by Fast Magic-Angle Spinning and Double-Quantum <sup>1</sup>H Solid-State NMR Spectroscopy. *J. Am. Chem. Soc.*, 1999, 121(28): 6712–6718
2. McMahon C.A., Hawrylak B., Palepu R., Calorimetric and NMR Investigations of the Micellar Properties of Sodium Dodecyl Sulfate in Aqueous Mixtures of Isomeric Butanediols. *Langmuir*, 1999, 15(2): 429–436
3. Markey L., Stievenard D., Devos A., Lannoo M.; Demol F.; de Backer M., STM observations of self-assembled 1D and 2D nanoclusters of aromatic cryptand molecules deposited on highly oriented pyrolytic graphite. *Supramole Science*, 1997, 4(3–4): 375–379

4. Huang Yaoxiong, Tan Runchu, Li Yonglong, Yang Yuquan, He Oicai, Effect of Salts on the Formation of C8-Lecithin Micelles in Aqueous Solution. *J. Colloid and Interface Sci.*, 2001, 236(1): 28–34
5. Miguel M. G., Burrows H. D., Formosinho S. J., Lindman, B., Fluorescence studies of polymer-surfactant association. *J. Mol. Struct.*, 2001, 563(1): 89–98
6. Lam Y. M., Goldbeck-Wood G., Mesoscale simulation of block copolymers in aqueous solution: parameterisation, micelle growth kinetics and the effect of temperature and concentration morphology. *Polymer*, 2003, 44(12): 3593–3605
7. Li Youyong., Guo Senli., Wang Kaixuan., Xu Xiaojie., Mesoscale computer simulation and its applications, *Progress in Chemistry*, 2000, 12(4) 361–375 ( in Chinese)
8. Hansson P., Schneider S., Lindman B., Phase separation in polyelectrolyte gels interacting with surfactants of opposite charge. *J. Phys. Chem. B.*, 2002, 106(38): 9777–9793
9. Yuan Shiling, Cai Zhengting, Xu Guiying, Mesoscopic simulation of aggregates in surfactant/oil/water systems. *Chinese Journal of Chemistry*, 2003, 21(2): 112–116 (in Chinese)
10. Yuan Shiling., Cai Zhengting., Xu Guiying., Dynamic simulation of aggregation morphology in surfactant solutions. *Acta Chimica Sinica*(in Chinese), 2002, 60(4), 241–245
11. Claesson P.M., Fielden M.L., Interactions between a 30 Charged Polyelectrolyte and an Anionic Surfactant in Bulk and at a Solid-Liquid Interface. *J. Phys. Chem. B.*, 1998, 102(7): 1270–1278
12. Groot R.D., Mesoscopic Simulation of Polymer-Surfactant Aggregation. *Langmuir*, 2000, 16(19): 7493–7502
13. Asefa T., Maclachlan M. J., Coombs N., Ozin, G. A., Periodic mesoporous organosilicas with organic groups inside the channel walls. *Nature*, 1999, 402(6764): 867–881
14. Zhang Jinli, Li Wei, Meng, Xiang-kun, Wang, Li, Zhu Li. Synthesis of mesoporous silica membranes oriented by self-assemblies of surfactants. *Journal of Membrane Science*, 2003, 222(1–2): 219–224

Front. Chem. China (2006)  
DOI 10.1007/s11458-006-0072-3

## ERRATUM

Ma Hua, Tao Zhanliang, Gao Feng, Chen Jun, Yuan Huatang

# Synthesis, characterization and hydrogen storage capacity of MS<sub>2</sub> (M = Mo, Ti) nanotubes

© Higher Education Press and Springer-Verlag 2006

Front. Chem. China (2006) 3: 260–264

Due to typesettings production errors, some mistakes were made. The Editorial Office regrets these errors.

- 1) p.261, Eq. (1) 300 should be changed to 300°C;
- 2) p.261, Eq. (2) 750 should be changed to 750°C;
- 3) p.262, the positions of the photos in Fig.2 and Fig. 3 should be exchanged.

The online version of the original article can be found at [http:// dx.doi.org/10.1007/s11458-006-0039-4](http://dx.doi.org/10.1007/s11458-006-0039-4)